1x3 beam splitter for TE polarization based on self-imaging phenomena in photonic crystal waveguides

Zhang, Min; Malureanu, Radu; Krüger, Asger Christian; Kristensen, Martin

Published in:
Optics Express

Link to article, DOI:
10.1364/OE.18.014944

Publication date:
2010

Document Version
Publisher's PDF, also known as Version of record

1x3 beam splitter for TE polarization based on self-imaging phenomena in photonic crystal waveguides

Min Zhang,[1,*] Radu Malureanu,[2] Asger Christian Krüger,[1] and Martin Kristensen[3]

[1]*Interdisciplinary Nanoscience Center, Aarhus University, Ny Munkegade 120, DK-8000 Århus C, Denmark*
[2]*Plasmonics and Metamaterials group, Department of Photonics Engineering, Technical University of Denmark*
[3] *Aarhus School of Engineering and Department of Physics and Astronomy, Aarhus University, Ny Munkegade 120, DK-8000 Århus C, Denmark*
minz@inano.dk

Abstract: Based on inspiration from multi-mode interference self-imaging and theoretical FDTD simulations, a 1x3 beam splitter was designed, fabricated and characterized. Measurements show that for TE-polarized incident light the power is distributed equally between the output ports within 1dB in the range from 1541nm to 1552nm, and the total transmission of the 1x3 splitter is equal to the corresponding length of a single-line-defect PhCW within the measurement uncertainty.

OCIS codes: (230.7390) Waveguides, planar; (130.5296) Photonic Crystal waveguides; (130.3120) Integrated optics devices; (999.9999) Self-imaging; (999.9999) multi-mode interference; (999.9999) e-beam lithography

References and links

1. G. Lifante, *"Integrated Photonics: Fundamentals"* (John Wiley & Sons Ltd, Chichester, 2005).
2. J. D. Joannopoulos, S. G. Johnson, J. N. Winn, and R. D. Meade, *"Photonic Crystals: Molding the Flow of Light (second edition)"* (Princeton University Press, Princeton, 2007), Chap. 8.
3. I. Park, H. S. Lee, H. J. Kim, K. M. Moon, S. G. Lee, B. H. O, S. G. Park, and H. Lee, "Photonic crystal power-splitter based on directional coupling," Opt. Express **12**(15), 3599–3604 (2004), http://www.opticsinfobase.org/abstract.cfm?URI=oe-12-15-3599.
4. T. B. Yu, M. H. Wang, X. Q. Jiang, Q. H. Liao, and J. Y. Yang, "Ultracompact and wideband power splitter based on triple photonic crystal waveguides directional coupler," J. Opt. A, Pure Appl. Opt. **9**(1), 37–42 (2007).
5. S. Boscolo, M. Midrio, and T. F. Krauss, "Y junctions in photonic crystal channel waveguides: high transmission and impedance matching," Opt. Lett. **27**(12), 1001–1003 (2002), http://www.opticsinfobase.org/abstract.cfm?URI=ol-27-12-1001.
6. S. H. Fan, S. G. Johnson, J. D. Joannopoulos, C. Manolatou, and H. A. Haus, "Waveguide branches in photonic crystals," J. Opt. Soc. Am. B **18**(2), 162–165 (2001).
7. Y. Zhang, Z. J. Li, and B. J. Li, "Multimode interference effect and self-imaging principle in two-dimensional silicon photonic crystal waveguides for terahertz waves," Opt. Express **14**, 2679–2689 (2006), ttp://www.opticsinfobase.org/abstract.cfm?URI=oe-14-7-2679.
8. T. Liu, A. R. Zakharian, M. Fallahi, J. V. Moloney, and M. Mansuripur, "Multimode interference-based photonic crystal waveguide power splitter," J. Lightwave Technol. **22**(12), 2842–2846 (2004).
9. A. Têtu, M. Kristensen, L. H. Frandsen, A. Harpøth, P. I. Borel, J. S. Jensen, and O. Sigmund, "Broadband topology-optimized photonic crystal components for both TE and TM polarizations," Opt. Express **13**(21), 8606–8611 (2005), http://www.opticsinfobase.org/oe/abstract.cfm?uri=OE-13-21-8606.
10. P. I. Borel, L. H. Frandsen, A. Harpoth, M. Kristensen, J. S. Jensen, and O. Sigmund, "Topology optimised broadband photonic crystal Y-splitter," Electron. Lett. **41**(2), 69–71 (2005).
11. L. H. Frandsen, P. I. Borel, Y. X. Zhuang, A. Harpøth, M. Thorhauge, M. Kristensen, W. Bogaerts, P. Dumon, R. Baets, V. Wiaux, J. Wouters, and S. Beckx, "Ultralow-loss 3-dB photonic crystal waveguide splitter," Opt. Lett. **29**(14), 1623–1625 (2004).
12. L. B. Soldano, and E. C. M. Pennings, "Optical multimode interference devices based on self-imaging - principles and applications," J. Lightwave Technol. **13**(4), 615–627 (1995).
13. H. J. Kim, I. Park, B. H. O, S. G. Park, H. Lee, and S. G. Lee, "Self-imaging phenomena in multi-mode photonic crystal line-defect waveguides: application to wavelength de-multiplexing," Opt. Express **12**(23), 5625–5633 (2004), http://www.opticsinfobase.org/oe/abstract.cfm?URI=OPEX-12-23-5625.
14. Z. J. Li, Y. Zhang, and B. J. Li, "Terahertz photonic crystal switch in silicon based on self-imaging principle," Opt. Express **14**(9), 3887–3892 (2006), http://www.opticsinfobase.org/abstract.cfm?URI=oe-14-9-3887.

#126338 - $15.00 USD Received 14 Apr 2010; revised 14 Jun 2010; accepted 22 Jun 2010; published 29 Jun 2010

15. H. B. Chen, Y. Xu, J. L. He, and Z. Hong, "A polarization splitter based on self-imaging phenomena in an anisotropic photonic crystal with an absolute photonic band gap," Opt. Commun. **282**(17), 3626–3629 (2009).
16. T. B. Yu, H. F. Zhou, Z. Gong, J. Y. Yang, X. Q. Jiang, and M. H. Wang, "Ultracompact multiway beam splitters using multiple coupled photonic crystal waveguides," J. Phys. D Appl. Phys. **41**(9), 095101 (2008).
17. O. Bryngdah, "Image formation using self-imaging techniques," J. Opt. Soc. Am. **63**(4), 416–419 (1973).
18. R. Ulrich, "Image-formation by phase coincidences in optical-waveguides," Opt. Commun. **13**(3), 259–264 (1975).
19. J. M. Heaton, R. M. Jenkins, D. R. Wight, J. T. Parker, J. C. H. Birbeck, and K. P. Hilton, "Novel 1-to-N way integrated optical beam-splitters using symmetrical mode mixing in GaAs/AlGaAs multimode wave-guides," Appl. Phys. Lett. **61**(15), 1754–1756 (1992).
20. G. P. Agrawal, *"Fiber-Optic Communication Systems"* (Wiley-Interscience, Rochester, 1997), Chap. 2.
21. L. H. Frandsen, A. V. Lavrinenko, J. Fage-Pedersen, and P. I. Borel, "Photonic crystal waveguides with semi-slow light and tailored dispersion properties," Opt. Express **14**(20), 9444–9450 (2006), http://www.opticsinfobase.org/abstract.cfm?URI=oe-14-20-9444.

1. Introduction

Large-scale Photonic Integrated Circuits (PICs), possess significant advantages by simplifying the optical system design, improving its reliability and reducing the space and power consumption [1]. Some of the most successful PIC structures are made from slab Photonic Crystals (PhCs) due to the ease of fabrication by using well-known lithographic techniques [2]. In such Photonic Crystal Waveguides (PhCWs), the optical field is confined, horizontally, by a photonic band-gap (PBG) provided by the PhC and, vertically, by total internal reflection due to the refractive index differences between different layers. Beam splitters are one of the central building blocks among the integrated components in PICs. These have been made by slab PhC [3–11], including Y-junctions [9–11], T-junctions [5, 6] and directional couplers [3, 4]. Until now, most of the work has focused on the performance of single-mode PhCW, but introducing multi-mode interference regions in the PhCWs provides new extraordinary characteristics [12] and some 1x2 components that use multimode interference have been proposed [7, 8].

In recent years, there has been a growing trend in the application of multimode interference (MMI) effects in integrated optics. Several components have been investigated theoretically including: a wavelength de-multiplexer based on self-imaging phenomena in PhCWs [13], the operation of a terahertz switch based on the self-imaging principle in silicon triangular PhCW [7, 14], TE and TM polarization splitters based on the simulation using self-imaging phenomena in PhCW [15] and a 1x2 splitter based on self-imaging phenomena in PhCWs [8]. The 2D simulation of Yu *et al.* [4, 16] indicated that the self-imaging phenomena also occurs in PhCWs between every second line defect in devices with many defect lines allowing the realization of 1xN (N≥2) splitters. Components based on every-other line-defect PhCWs are ultra-compact. The beat-length in the MMI region is much shorter than in the MMI region of conventional photonic waveguides. Moreover, in the latter the adjacent output waveguides have to be separated far enough to minimize coupling between them, and generally a rather wide multi-mode section is required. The every-other line-pattern in the former also facilitates the multi-mode field distribution [16]. The layout of rod slabs was adapted in Yu *et al.*'s research, but high transmittance can be obtained only for very long rods, increasing the fabrication difficulty. In contrast, thin air-slab PhCW devices with high transmittance can be easily fabricated and integrated with other PIC building blocks. Standard SOI wafers and e-beam lithography provide our fabrication platform. Here we report the theoretical and experimental results of a 1x3 beam splitter based on self-imaging in the 340nm top silicon layer of a SOI wafer.

2. Self-imaging principle and theoretical simulation

Bryngdahl *et al.* were the first suggesting the possibility of achieving self-imaging in slab waveguides [17] and Urich *et al.* explained the principle in detail [18]. Self-imaging is a property of multi-mode waveguides by which an input field profile is reproduced in single or multiple images at periodic intervals along the propagation direction [12, 19].

#126338 - $15.00 USD Received 14 Apr 2010; revised 14 Jun 2010; accepted 22 Jun 2010; published 29 Jun 2010

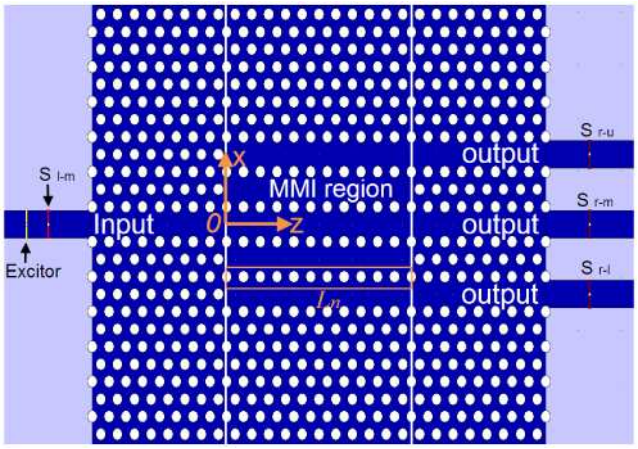

Fig. 1. Schematic layout of 1x3 beam splitter consisting of input, MMI and output PhCWs. The excitor and sensors for the FDTD simulation are arranged in the ridge waveguides.

The 2D PhC is formed by a triangular configuration with lattice pitch of Λ=380 nm and air hole diameter of D=222nm. This PhC structure defined in silicon (refractive index n=3.476) gives rise to high transmittance and a photonic band-gap (PBG) at near-infrared wavelength. The PBGs are disallowed bands in which the wavelengths are unable to pass through the PhC. Using a line-defect PhCW, light that propagates in the waveguide with a wavelength within the band-gap of the crystal is confined to the defect, and can be directed along the defect from one location to another. A W1 waveguide is obtained by removing exactly one single row of air-holes in the *Γ-K* direction of the lattice. Our proposed slab PhCW 1x3 beam splitter is shown in Fig. 1. It consists of three sections: a single-mode input, the MMI region, and three single-mode outputs all along the *Γ-K* direction. The lengths of the input and output ports are fixed in our theoretical design. The length L_n of the MMI region needs to be optimized and corresponds to the length of *n* lattices in MMI region (*n* must be an integer to preserve the crystal structure). The interference between adjacent output ports can be ignored because they are short and separated by three rows of air holes. Only TE polarization was calculated in the simulation, considered as TE-like in 3D simulation. The TE-like modes are even (symmetric) and odd (anti-symmetric) about the mirror-symmetry plane(x = 0). The symmetric interference is adopted based on the principle of symmetry matching [19].

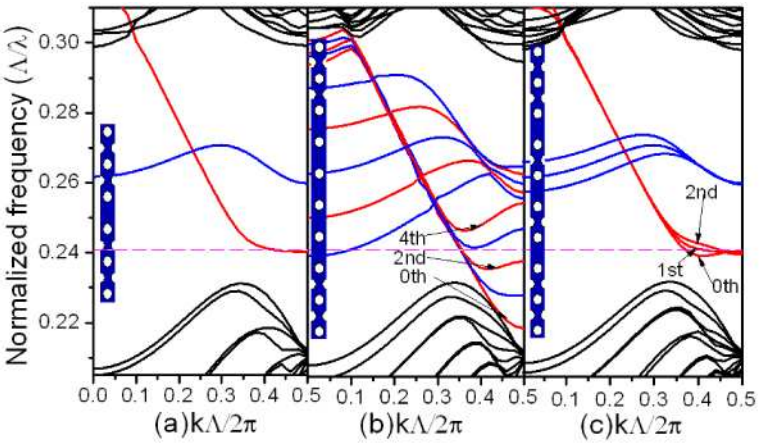

Fig. 2. Dispersion diagram for TE polarization of the PhCWs calculated using 3D PWE method. The supercells are shown in the insets. The black lines are PhC modes, while the red (blue) lines are even (odd) gap-guided modes.

#126338 - $15.00 USD Received 14 Apr 2010; revised 14 Jun 2010; accepted 22 Jun 2010; published 29 Jun 2010

Figure 2 presents the in-plane normalized dispersion diagrams for single- and multi-mode PhCWs calculated by 3D plane wave expansion (PWE) method with the grid spacing of Λ/16. Super-cells are depicted as inserts. Single-mode W1 PhCWs support one even mode (Fig. 2a) and multi-mode PhCWs support five and three even modes (Fig. 2b and Fig. 2c) in MMI region and output region. The bottom of the single-mode frequency span is very close to that of the multi-mode counterpart in the output region. This means that a 1x3 beam splitter is conceivable in this slab design near the normalized frequency of 0.241 (Λ/λ) in order to obtaining high transmittance [11, 21]. Figure 3 shows the transverse profile of the magnetic field H_y for these even modes of the supercells at kΛ/2π=0.5, calculated by 2D PWE method. All the even multi-modes are symmetric through the x=0 plane. Only the modes corresponding to the identical frequency can be excited (see the pink line in Fig. 2). However, it is possible to excite a superposition of modes at the excitation frequency.

The configuration of Fig. 1 is directly used in 3D FDTD modeling with the grid spacing of Λ/24. Different L_n's were simulated numerically. The simulations show that the components with L_n=10Λ and 11Λ split the input power equally and exhibit vey good transmittance. This means that theoretically the first 3-fold images are obtained due to MMI, between 10Λ and 11Λ. The net normalized transmittance is obtained by the net transmittance through the theoretical sensors in the right ridge waveguides divided by that through the input sensor in the left waveguide. These transmittances for the W1 PhCW and the 1x3 splitter with L_n=11Λ are shown in Fig. 4a. From the FDTD simulation, the optimum wavelength is 1567.4 nm and the total normalized transmittance is close to that for a W1 PhCW. A H_y field distribution at 1567.4 nm through the same 1x3 splitter is depicted in Fig. 4b.

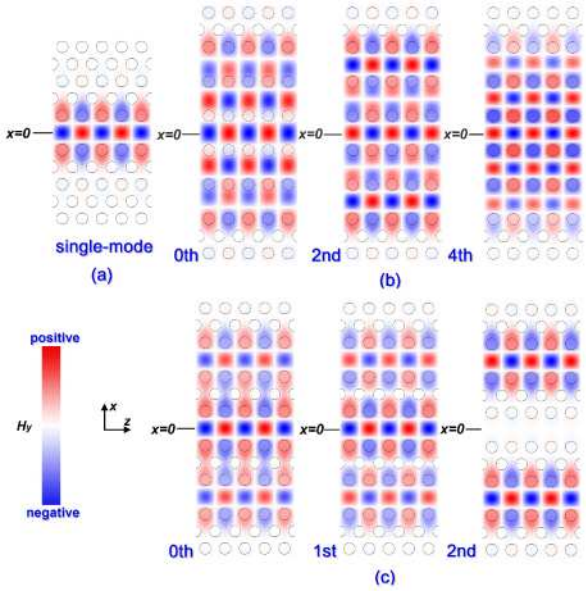

Fig. 3. The transverse profile of the magnetic field H_y for the even modes at kΛ/2π=0.5, a) input-, b) MMI- and c) output-region.

The variation in dispersion and thereby the wavelength-dependent transmittance through each of the output ports can be explained through the variation of the group velocity v_g of light with frequency ω in the optical waveguide given as Eq. (1) [20]:

$$v_g = \frac{d\varpi}{dk} = \frac{c_0}{n_g} \tag{1}$$

where k is the wavevector along the waveguide, n_g the group index.

#126338 - $15.00 USD Received 14 Apr 2010; revised 14 Jun 2010; accepted 22 Jun 2010; published 29 Jun 2010

The dispersion properties of a very similar W1 PhCW have been discussed by *L.H. Frandsen* [21]. The even PBG mode is seen from Fig. 2a to be flat from k_z=0.35 to 0.5. The variation approaches zero in this range, addressed as the slow-light regime. The even semi-slow PBG mode penetrates into the photonic crystal cladding; and is therefore especially sensitive to the presence of the adjacent two rows of holes. In our devices, the structures of the input and each of output ports still maintain the character of the W1 PhCW. The input field is well matched to the PhCW and only guided modes will be excited in the component based on symmetric interference [19]. The second line is removed in the MMI region to permit self-imaging, so the modal field can distribute at every-other line-defect (Fig. 3b) and form maxima at the end of the MMI region. The distribution of the modal field in MMI region depends on the position and input frequency introduced from the single-mode port. After the coupling into the MMI region, the modal field around 1567.4 nm is distributed equally after propagating approximately 11Λ leading to the first three-fold imaging (Fig. 4b).

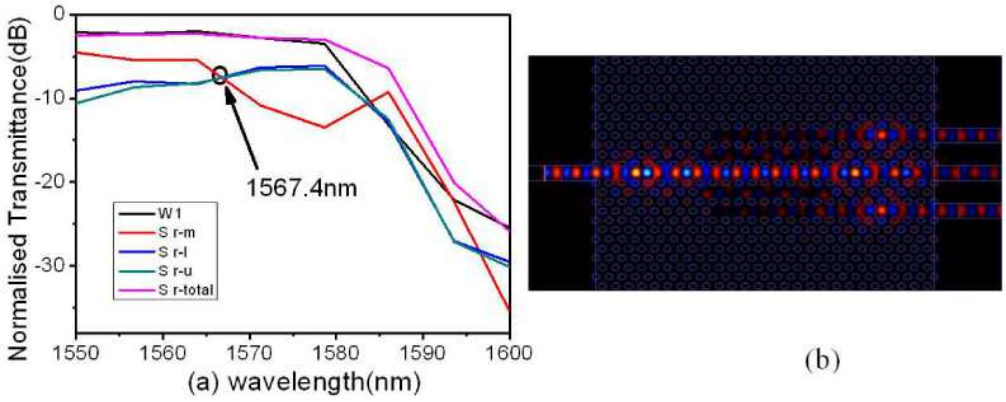

Fig. 4. (a) Simulated normalized TE-polarized transmittance by 3D FDTD for the splitter with Ln=11Λ, (b) A snapshot of H_y at 1567.4 nm.

3. Fabrication and characterization

The designed splitters with different L_n have been fabricated using e-beam lithography (JEOL- JBX9300FS) and inductively coupled plasma etching (ICP). In this way the desired design was defined into a 340-nm silicon layer. A SEM micrograph of the splitter with L_n=11Λ is shown in Fig. 5a. The air holes have a diameter of 220 +/– 5nm. The width of the ridge waveguides connected to/from the splitters is 0.53μm. The upper and lower output waveguides are separated from the central output waveguide using cosine bends after 5μm length in order to avoid coupling between the adjacent ridge waveguides (shown in Fig. 5b). Straight tapers expand the waveguides to/from 4μm diameter into and out of the PhCWs.

The device under test (DUT) has been characterized with the setup illustrated in Fig. 5c. Light is generated with an Agilent 83437A Broadband (LED) Source, and lensed fibers are used to focus the light into and out of the DUT. Finally, the light was detected by an ANDO AQ6315 Optical Spectrum Analyzer using a resolution of 2nm.

The normalized transmittance spectra for TE polarization from 1480 to 1580 nm are characterized. The 1x3 splitters with L_n from 10Λ to 13Λ can divide the incident light into three output channels in some wavelength span. Among them, the splitter with L_n=11Λ is the best. The normalized 11Λ TE-polarized spectra are shown in Fig. 6a. The input power after the splitter is divided equally into three parts between 1541 and 1552 nm, with a maximum difference below 1dB. The experimental result is consistent with that of the numerical modeling. The small difference is attributed to the finite grid and omission of the native oxide in the modeling and fabrication errors. The total output of the 1x3 splitter is close to a W1 PhCW with the same length. Especially for the wavelength below 1550nm, the loss compared to W1 PhCW is within the measurement uncertainty.

#126338 - $15.00 USD Received 14 Apr 2010; revised 14 Jun 2010; accepted 22 Jun 2010; published 29 Jun 2010

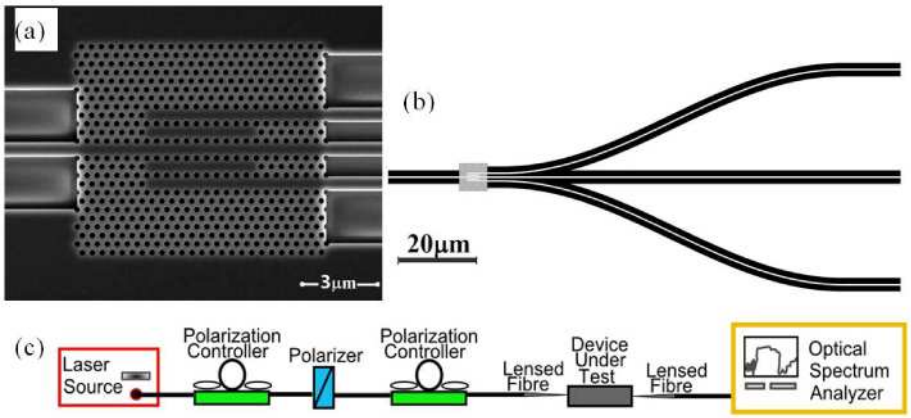

Fig. 5. (a) SEM micrograph of the splitter with Ln=11Λ, (b) ridge waveguides connected to the splitter, (c) Schematic diagram of the measurement setup.

When the L_n=11Λ splitter is reversed, it works as a 3x1 combiner. The incident light reaches the component from the side with three output ports. Figure 6b shows the normalized transmittance spectra through each port. Because the total power is induced separately from each port, the total input power is around 4.8dB higher than the total output power. Since two of the spectra are almost identical, it illustrates the possibility for realizing further multiple functionality.

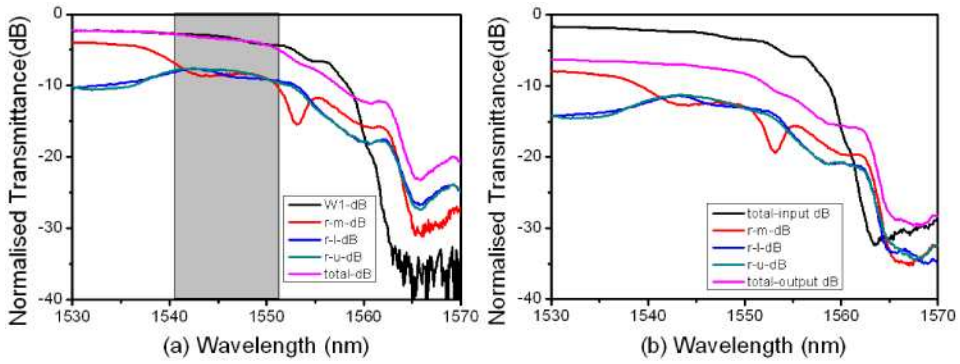

Fig. 6. (a) Measured normalized TE-polarized transmittance for the 1x3 splitter with *Ln*=11Λ. (b) Measured normalized TE-polarized transmittance (dB) for the device operating as a 3x1 combiner with the reversed transmittance direction.

4. Conclusion

In conclusion, we have presented a 1x3 splitter with excellent performance for TE polarization. It splits the input power equally into three output ports within a ~10nm range near 1550nm. The reversed performance as a 3x1 combiner is consistent with the former. If the 1x3 and 3x1 functions are used together, more functions can be obtained, for instance the 3x3 function for qutrit, which is in progress in our group.

Acknowledgments

This work was supported mainly by The Danish Agency for Technology and Innovation (NABIIT) through the project 'Mobile quantum Security' (MOBISEQ), and partly by the Danish Technical Research Council through the research program 'Planar Integrated PBG Elements' (PIPE).

#126338 - $15.00 USD Received 14 Apr 2010; revised 14 Jun 2010; accepted 22 Jun 2010; published 29 Jun 2010